AGU PUBLICATIONS

Geophysical Research Letters

RESEARCH LETTER
10.1002/2016GL070021

**Key Points:**
- Fiordland sediment accumulation rates are high near land and sea interfaces and low in medial areas, away from primary sediment sources
- The organic content of modern Fiordland sediments is diluted and shielded from surface processes by mineral sediment accumulation
- The delivery mechanism of sediment sets the initial OC content of the sediment and future preservation potential

**Supporting Information:**
- Supporting Information S1

**Correspondence to:**
M. T. Ramirez,
mramire1@tulane.edu

**Citation:**
Ramirez, M. T., M. A. Allison, T. S. Bianchi, X. Cui, C. Savage, S. E. Schüller, R. W. Smith, and L. Vetter (2016), Modern deposition rates and patterns of organic carbon burial in Fiordland, New Zealand, *Geophys. Res. Lett.*, *43*, 11,768–11,776, doi:10.1002/2016GL070021.

Received 17 JUN 2016
Accepted 6 NOV 2016
Accepted article online 9 NOV 2016
Published online 26 NOV 2016



# Modern deposition rates and patterns of organic carbon burial in Fiordland, New Zealand

**Michael T. Ramirez[1], Mead A. Allison[1,2], Thomas S. Bianchi[3], Xingqian Cui[3], Candida Savage[4,5], Susanne E. Schüller[4,6], Richard W. Smith[7], and Lael Vetter[1]**

[1]Department of Earth and Environmental Sciences, Tulane University, New Orleans, Louisiana, USA, [2]The Water Institute of the Gulf, Baton Rouge, Louisiana, USA, [3]Department of Geological Sciences, University of Florida, Gainesville, Florida, USA, [4]Department of Marine Science, University of Otago, Dunedin, New Zealand, [5]Department of Biological Sciences, University of Cape Town, Cape Town, South Africa, [6]Now at Inter-Research Science Center, Oldendorf/Luhe, Germany, [7]Global Aquatic Research, LLC, Sodus, New York, USA

**Abstract** Fjords are disproportionately important for global organic carbon (OC) burial relative to their spatial extent and may be important in sequestering atmospheric $CO_2$, providing a negative climate feedback. Within fjords, multiple locally variable delivery mechanisms control mineral sediment deposition, which in turn modulates OC burial. Sediment and OC sources in Fiordland, New Zealand, include terrigenous input at fjord heads, sediment reworking over fjord-mouth sills, and landslide events from steep fjord walls. Box cores were analyzed for sedimentary texture, sediment accumulation rate, and OC content to evaluate the relative importance of each delivery mechanism. Sediment accumulation was up to 3.4 mm/yr in proximal and distal fjord areas, with lower rates in medial reaches. X-radiograph and $^{210}$Pb stratigraphy indicate mass wasting and surface-sediment bioturbation throughout the fjords. Sediment accumulation rates are inversely correlated with %OC. Spatial heterogeneity in sediment depositional processes and rates is important when evaluating OC burial within fjords.

## 1. Introduction

Organic carbon (OC) burial in marine sediments has been recognized as a driver of long-term dynamics in the global carbon cycle, as well as a control on atmospheric $CO_2$ concentrations [*Berner*, 2003; *Mackenzie and Lerman*, 2010]. Characterizing the rate and nature of sediment accumulation in areas of high OC burial is key to advancing understanding of global carbon dynamics. Fjords can function as hot spots of OC burial and preservation due to high OC input and sediment accumulation. Recent work has highlighted high rates of OC burial in fjords around the world (up to 11% of annual global marine OC burial) [*Smith et al*., 2015], despite their disproportionately small global surface area, with OC burial rates up to 1000 times greater than other continental margin environments [*Hinojosa et al*., 2014]. The OC buried in fjords is a combination of (1) marine biogenic material, (2) biogenic production in the fjord, and (3) terrigenous OC from catchment slopes [*Syvitski et al*., 1990; *Schüller et al*., 2015; *Cui et al*., 2016]. Rapid sediment deposition reduces the duration of exposure of sedimentary OC to surface processes and postdepositional decomposition in situ [*Burell*, 1988; *St-Onge and Hillaire-Marcel*, 2001; *Nuwer and Keil*, 2005; *Smith et al*., 2010; *Cui et al*., 2016], which is dependent on oxygenation and burial rate. Thus, high rates of mineral deposition may enhance OC storage.

Fjords occur over a range of latitudes (40° to 80°N and S [*Pickrill*, 1987]) and climate zones and are subject to a variety of sediment delivery mechanisms [*Bianchi*, 2007]. Biogenic production, benthic reworking, and suspended-sediment flocculation may occur throughout fjords [*Pickrill*, 1987]. Other delivery mechanisms tend to be localized and tied to position within the fjord system, including glacial meltwater and ice transport [*Powell and Molnia*, 1989; *Hein and Syvitski*, 1992], input of coarse sediment from fjord-head rivers [*Syvitski and Murray*, 1981; *Bogen*, 1983; *Bentley and Kahlmeyer*, 2012], landslides along steep walls [*Aarseth et al*., 1989; *Hjelstuen et al*., 2013], and tidal and wave-driven advection at marine margins [*Pickrill*, 1987; *Inall and Gillibrand*, 2010]. Over millenial time scales during the Holocene, the thickest sediment deposits appear to build up in the deep, flat, central basins of fjord systems [*Aarseth et al*., 1989; *Bentley and Kahlmeyer*, 2012; *Hjelstuen et al*., 2013].

For fjords worldwide, *Syvitski et al*. [1990] identify four sources of OC: terrigenous detritus (particularly in temperate, vegetated fjords), macrophytic algae and marsh detrital production, marine snow, and epilithic

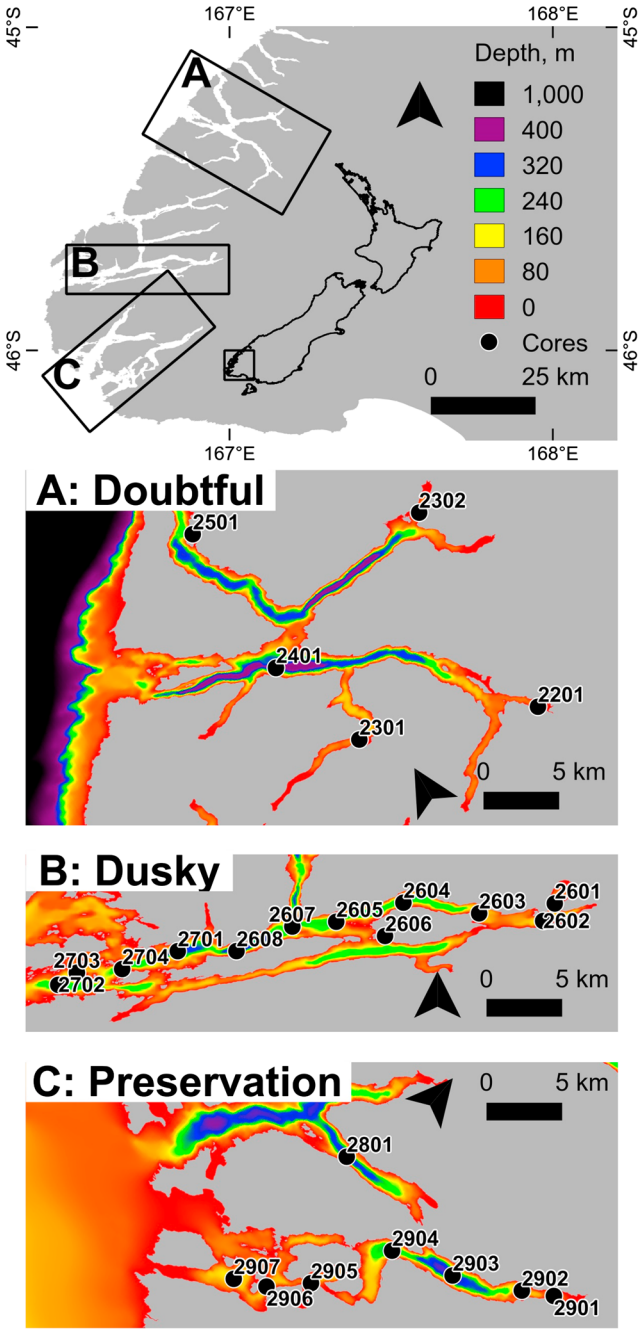


**Figure 1.** Maps of the studied fjords, including the locations of box cores in (a) Doubtful Sound, (b) Dusky Sound, and (c) Preservation Inlet. Bathymetry was interpolated from navigational charts published by Land Information New Zealand [2001].

production. Upon entering the fjord, particulate OC is subject to range of hydrologic and physical processes that dictate the spatial distribution of its accumulation [*Syvitski et al.*, 1985]. In these dynamic systems where OC is preferentially sequestered, it is particularly important to constrain the relationship between sediment and OC accumulation rates.

Fiordland, New Zealand, is at a low latitude (~46°S) compared to other fjord regions and is not significantly glaciated [*Pickard and Stanton*, 1980; *Pickrill*, 1987]. Thus, these fjords are affected by different primary sedimentary drivers than high-latitude, glaciated fjords. Westerly winds bring oceanic moisture and orographic precipitation over the Southern Alps (>6 m/yr) [*Sansom*, 1984; *Pickrill*, 1987; *Knudson et al.*, 2011]. The high volume of precipitation, combined with episodic, seismically induced landslides, transports mineral and organic sediment from steep, vegetated catchments of Fiordland to the deep (often >100 m) fjord basins [*Hancox and Perrin*, 2009; *Smith et al.*, 2015; *Cui et al.*, 2016].

To date, a comprehensive examination of controls on the spatial variability in sediment and OC accumulation rates across these fjords has not been conducted. Here we build on previous work in Fiordland, New Zealand [*Smith et al.*, 2010; *Schüller and Savage*, 2011; *Schüller et al.*, 2013; *Hinojosa et al.*, 2014; *Schüller et al.*, 2015; *Smith et al.*, 2015; *Cui et al.*, 2016], utilizing geochronology, textural analyses, and OC measurements to infer the sediment delivery mechanisms operating in different regions of the fjords, and their control on the rates and geographic distribution of modern OC burial. Fiordland—and fjords, in general—is a region of gradients: in topography, climate, and sedimentary input, and we hypothesize that the rates of sediment deposition throughout the fjords reflect the gradients in delivery mechanisms that brought them there. We compare the calculated sediment accumulation rates and inferred delivery mechanisms with those previously published for Fiordland, as well as to the total thicknesses of postglacial sediment observed in previous studies of these fjords. In the context of fjords in other global regions, we suggest that other fjord regions—which are currently glaciated—may trend toward the conditions presently observed in modern Fiordland with future climate change.

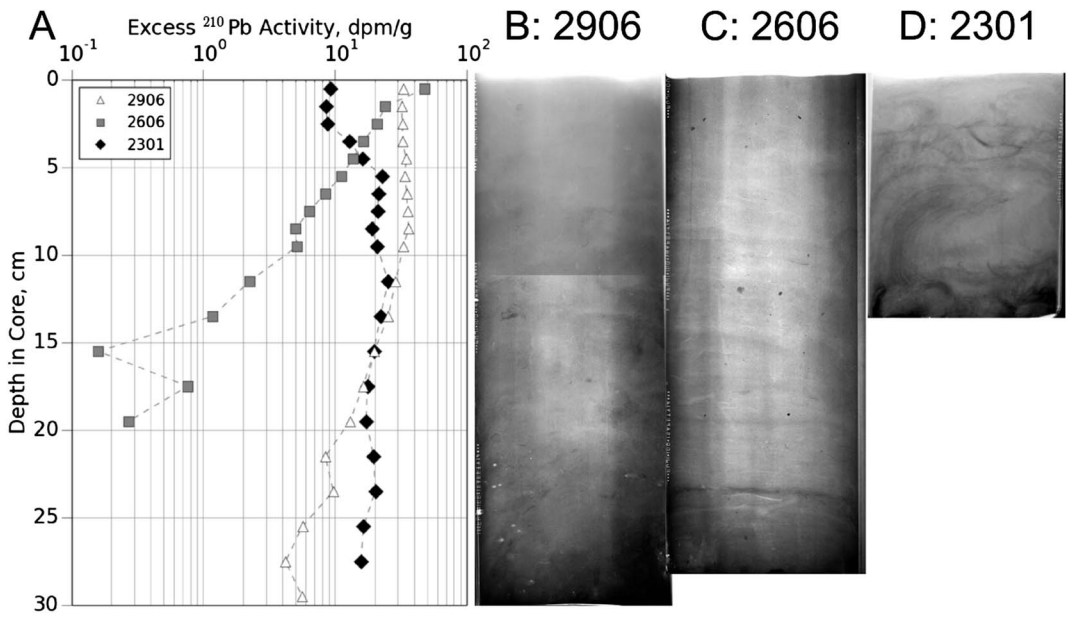


**Figure 2.** (a) Excess $^{210}$Pb profiles and X-radiographs of (b) core 2906 from near the mouth of Preservation inlet, (c) core 2606 from an isolated basin in Dusky Sound, and (d) core 2301 from Doubtful Sound, displaying chaotic structure.

## 2. Methods

Thorough descriptions of all field and laboratory method and calculations are given in Supporting Information S1.

## 3. Results

### 3.1. Mineral Sediment Granulometry

Grain size measurements are fully reported as the D10, D50, and D90 (10th, 50th, and 90th grain diameter percentiles, respectively) in Table S1 and Figure S1 in the supporting information. All samples are classified as silty clays and clayey silts, with respective mean D10, D50, and D90 of 1.4, 9.1, and 37.0 μm for all samples ($n = 25$). No samples contained more than 10% sand-sized material, except for large woody particles and shell fragments removed by sieve prior to granulometric analysis. Median grain size variability was minimal within any core; for example, the largest standard deviation in D50 grain size within a core was 2.0 μm ($n = 4$). Core 2601 showed the coarsest grain size, with a mean D50 grain size (i.e., mean of median grain sizes from all samples in the core) of 20.5 μm. This core was collected in proximal Dusky Sound (Figure 1), where high terrigenous input may be expected due to being located near the fjord-head Seaforth River delta. All other cores analyzed for grain size had median grain sizes that ranged between 6.1 and 9.3 μm, demonstrating a sharp dropoff in grain diameter away from proximal areas.

### 3.2. Box Core X-Radiography

For most cores (18 of 24), X-radiographs were characterized by relatively featureless (massive) or finely (millimeter-scale) laminated muds, occasionally with evidence of a bioturbated surface layer (upper ~8 cm thick in Figure 2b) with laminations disrupted by burrow traces overlying millimeter-scale laminated strata (apparent in Figure 2c). Even in massive intervals, some cores showed evidence of biological activity including macrofossils and burrow traces (shells and burrows; Table 1), consistent with diverse macrofaunal communities and a predominance of burrowing polychaetes in the fjords [*Brewin et al.*, 2008].

### 3.3. Box Core Pb-Geochronology

Twenty one of the 25 box cores exhibited $^{210}$Pb profiles characterized by a surface mixed layer (SML; thickness ranged 0–15.5 cm with a mean of 4.24 cm) overlying a logarithmic decay profile characteristic of steady state sediment accumulation on interannual time scales (cores 2606 and 2906; Figure 2a). Linear

**Table 1.** Downcore Analytical Results (Including Site Name, Location, and Water Depth) of Surface $^{210}$Pb Excess Activity (SPb_xs), Linear Sedimentation Rate (LSR) Calculated From $^{210}$Pb Regression, $R^2$ Value of the Regression Analysis Used to Calculate Linear Sedimentation Rate, Thickness of the Surface Mixed Layer (SML), Mass Accumulation Rate (MAR), Percent Organic Carbon (%OC), and Carbon Accumulation Rate (OCAR)

| Site | Lat (deg) | Long (deg) | Depth (m) | SPb_xs (dpm/g) | LSR (mm/yr) | $R^2$ | SML (cm)[a] | MAR (mg/cm$^2$/yr) | %OC | OCAR (mg/cm$^2$/yr) |
|---|---|---|---|---|---|---|---|---|---|---|
| 2201 | −45.458 | 167.154 | 93 | 18.76 ± 1.50 | 1.17 ± 0.07 | 0.87 | 1.5 ± 0.5 | 69 ± 4 | 5.43 ± 0.62 | 3.77 ± 0.03 |
| 2301 | −45.407 | 167.011 | 66 | 9.25 ± 1.09 | | 0.16 | | | 10.58 ± 0.76 | |
| 2302 | −45.266 | 167.15 | 71 | 12.69 ± 1.21 | 2.87 ± 0.61 | 0.9 | 5.5 ± 0.5 | 170 ± 36 | | |
| 2401 | −45.319 | 166.98 | 435 | 56.23 ± 3.91 | 3.39 ± 0.27 | 0.86 | 2.5 ± 0.5 | 205 ± 16 | 4.51 ± 0.35 | 9.23 ± 0.06 |
| 2501 | −45.187 | 166.975 | 17 | 4.53 ± 0.48 | | 0.14 | | | 0.87 ± 0.12 | |
| 2601 | −45.714 | 166.945 | 83 | 11.89 ± 0.94 | 2.06 ± 0.73 | 0.99 | 1.5 ± 0.5[a] | 122 ± 43 | 5.85 ± 0.32 | 7.12 ± 0.14 |
| 2602 | −45.729 | 166.936 | 168 | 24.33 ± 1.79 | 1.70 ± 0.13 | 0.79 | 1.5 ± 0.5 | 97 ± 8 | 7.62 ± 0.71 | 7.42 ± 0.06 |
| 2603 | −45.722 | 166.881 | 173 | 22.09 ± 1.58 | 2.65 ± 0.24 | 0.88 | 0.5 ± 0.5 | 157 ± 14 | | |
| 2604 | −45.713 | 166.816 | 257 | 39.48 ± 3.40 | 1.32 ± 0.10 | 0.97 | 1.5 ± 0.5 | 78 ± 6 | | |
| 2605 | −45.729 | 166.761 | 282 | 63.46 ± 5.24 | 1.06 ± 0.05 | 0.93 | 1.5 ± 0.5 | 62 ± 3 | | |
| 2606 | −45.741 | 166.801 | 33 | 47.84 ± 4.06 | 0.25 ± 0.01 | 0.98 | 0.5 ± 0.5 | 13 ± 1 | 11.44 ± 0.48 | 1.50 ± 0.003 |
| 2607 | −45.733 | 166.722 | 309 | 50.19 ± 4.24 | 0.69 ± 0.04 | 0.98 | 1.5 ± 0.5[a] | 41 ± 2 | | |
| 2608 | −45.755 | 166.677 | 305 | 66.02 ± 5.56 | 1.17 ± 0.05 | 0.95 | 2.5 ± 0.5[a] | 69 ± 3 | | |
| 2701 | −45.755 | 166.625 | 316 | 49.73 ± 4.19 | 1.56 ± 0.10 | 0.97 | 5.5 ± 0.5[a] | 92 ± 6 | | |
| 2702 | −45.783 | 166.523 | 235 | 40.24 ± 2.84 | 3.30 ± 0.72 | 0.87 | 3.5 ± 0.5[a] | 205 ± 58 | 2.86 ± 0.25 | 5.87 ± 0.11 |
| 2703 | −45.773 | 166.54 | 195 | 36.15 ± 3.10 | | 0.64 | | | | |
| 2704 | −45.769 | 166.578 | 266 | 45.33 ± 3.84 | 1.37 ± 0.19 | 0.96 | 7.5 ± 0.5[a] | 81 ± 11 | | |
| 2801 | −45.963 | 166.684 | 319 | 21.04 ± 1.60 | 1.91 ± 0.15 | 0.93 | 5.5 ± 0.5[a] | 113 ± 9 | | |
| 2901 | −45.941 | 166.896 | 70 | 6.90 ± 1.03 | | 0.69 | | | 9.23 ± 0.30 | |
| 2902 | −45.955 | 166.873 | 123 | 12.02 ± 1.37 | 1.85 ± 0.15 | 0.86 | 6.5 ± 0.5 | 109 ± 9 | | |
| 2903 | −45.983 | 166.819 | 336 | 18.16 ± 1.48 | 0.57 ± 0.04 | 0.96 | 10.0 ± 1.0 | 34 ± 2 | | |
| 2904 | −45.999 | 166.764 | 246 | 19.78 ± 1.61 | 0.56 ± 0.03 | 0.97 | 5.5 ± 0.5 | 33 ± 2 | | |
| 2905 | −46.065 | 166.729 | 133 | 11.78 ± 1.04 | 2.31 ± 0.16 | 0.79 | 0.5 ± 0.5[a] | 136 ± 9 | | |
| 2906 | −46.093 | 166.703 | 121 | 33.10 ± 2.91 | 1.47 ± 0.06 | 0.97 | 8.5 ± 0.5 | 87 ± 4 | | |
| 2907 | −46.104 | 166.678 | 144 | 27.02 ± 2.40 | 2.09 ± 0.17 | 0.97 | 15.5 ± 1.5[a] | 128 ± 10 | 3.59 ± 0.09 | 4.61 ± 0.01 |

[a]Visible evidence of bioturbation/macrofossils in the X-radiographs.

sedimentation rates (LSR) were able to be calculated for these cores according to the logarithmic decay methods in Supporting Information S1.

LSR for all cores ranged 0.25–3.4 mm/yr. Mean LSR calculated for Doubtful Sound (2.5 ± 0.3 mm/yr; $n = 3$) was greater than those of Dusky Sound (1.6 ± 0.2 mm/yr; $n = 11$) and Preservation Inlet (1.5 ± 0.1 mm/yr; $n = 7$). However, these differences are influenced by differences in spatial sampling coverage between fjords, as fewer cores were collected in the medial areas of Doubtful Sound. LSR (Figure 3) trends show maxima at the landward and seaward ends of each fjord and minima in the medial regions of the fjords, as observed in Dusky Sound and Preservation Inlet. Mean LSR for proximal areas, medial areas, and distal areas were 1.8 ± 0.3 mm/yr ($n = 9$), 1.0 ± 0.1 mm/yr ($n = 6$), and 2.2 ± 0.3 mm/yr ($n = 6$), respectively.

LSR could not be calculated from the excess $^{210}$Pb profiles in cores 2301, 2501, 2703, and 2901. Excess $^{210}$Pb profiles at these sites displayed downcore activity patterns ranging from scattered, to stepwise, to nearly uniform excess activities (Figure 2d). X-radiographs of these cores suggest landslide events (distorted bedding; Figure 2d) or highly bioturbated deposits (massive/featureless).

For the entire Fiordland region, we calculated a total sediment (see Supporting Information S1 for calculation details) accumulation rate of 750,098 T/yr (1012 T/km$^2$/yr).

### 3.4. Organic Carbon Content of Fiordland Sediments

Mean %OC for each core ranged 0.9–11.4%OC (Table 1). Within each fjord, a general down-fjord gradient of decreasing %OC was observed, with cores in proximal areas having a mean %OC of 7.7 % and cores in distal areas having a mean of 3.0 %OC. Only one medial-region core was analyzed for OC (Core 2606, Dusky Sound;

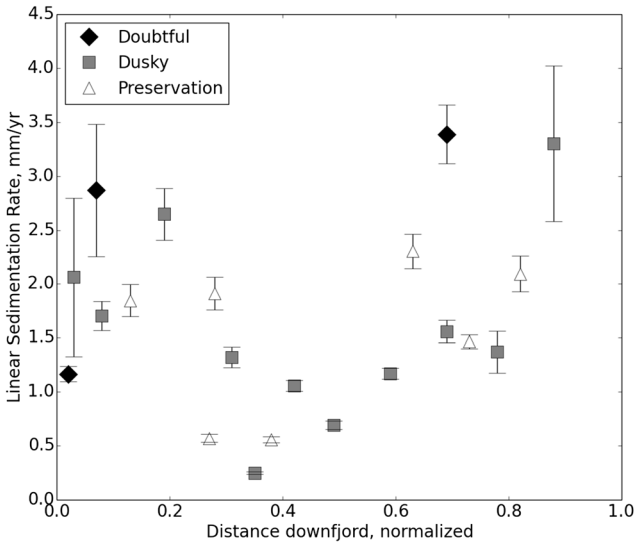


**Figure 3.** Linear sedimentation rates and locations for cores from Doubtful Sound, Dusky Sound, and Preservation Inlet.

Figure 1b), yielding an anomalously high (11.4%) OC; this core is from a restricted and shallow subbasin (Figure 1) with a small, relatively low-elevation catchment.

Three cores analyzed for %OC did not have $^{210}$Pb profiles suitable for LSR calculation: one from Preservation Inlet (core 2901) and two from Doubtful Sound (cores 2301 and 2501). Core 2901 from Preservation Inlet had a high (9.3%) OC concentration, and abundant bioturbation and macrofossils visible in the X-radiograph, suggesting that the irregular $^{210}$Pb profile in this core is the result of biological, not physical, mixing. The two Doubtful Sound cores nearly encompass the full range of %OC (Core 2301, proximal, 10.6 %OC, and Core 2501, distal, 0.9 %OC). The proximal core displayed a chaotic sedimentary fabric in the X-radiograph (Figure 2c) and a nearly uniform downcore $^{210}$Pb profile, both consistent with a mass movement (landslide) signature (i.e., apparently instantaneous deposition on $^{210}$Pb time scales). The distal core was not recorded by X-radiography but displays a similar, nearly uniform $^{210}$Pb profile.

### 3.5. Organic Carbon Accumulation Rates

Organic carbon accumulation rates (OCARs) ranged from $1.5 \pm 0.003$ to $9.2 \pm 0.1$ mg/cm$^2$/yr, with a mean of $5.6 \pm 0.1$ mg/cm$^2$/yr. For Doubtful Sound and Dusky Sound, mean OCAR were $6.5 \pm 0.04$ ($n = 2$) and $5.5 \pm 0.1$ ($n = 4$) mg/cm$^2$/yr, respectively. Preservation Inlet had one core with a calculated OCAR ($4.6 \pm 0.01$ mg/cm$^2$/yr). OCAR in Doubtful Sound increased from fjord head to mouth, while OCAR in Dusky Sound decreased from fjord head to mouth. LSR and %OC exhibit an inverse correlation, suggesting that large changes in LSR are primarily controlled by the mineral contribution.

A total Fiordland OC burial rate of 35,773 T/yr (50 T/km$^2$/yr) was calculated by using OCAR from the proximal, medial, and distal areas of the three southernmost fjords.

## 4. Discussion

### 4.1. Delivery Mechanisms for Fiordland Sediment

Sedimentological and stratigraphic investigations of fjords worldwide typically show the thickest Holocene sediment deposits in the deep, medial basins [*Aarseth et al.*, 1989; *Bentley and Kahlmeyer*, 2012; *Hjelstuen et al.*, 2013], suggesting that sediment delivery mechanisms favor sediment focusing in these subenvironments. In Fiordland, seismic studies conducted to date [*Pickrill et al.*, 1992; *Pickrill*, 1993] also show this sediment focusing in the central basins of the fjords sampled in the present study. However, the deep basins in these fjords fall within the medial region—a region that is experiencing the minimum LSR on $^{210}$Pb geochronological (~100 yr) time scales (Figure 3). If Figure 3 shows an anomalous spatial pattern of modern accumulation rates compared to sediment thickness, this implies that there has been either a change in the mechanisms delivering sediment to Fiordland compared to earlier in the Holocene or the rates of these mechanisms have changed.

Indeed, the LSR observed over $^{210}$Pb time scales in this study (0.25–3.39 mm/yr) are greater than those measured over $^{14}$C time scales previously in Fiordland (0.25–1.00 mm/yr [*Pickrill*, 1993] and 0.60–1.70 mm/yr [*Knudson et al.*, 2011]). It is possible that this LSR acceleration through the Holocene is reflective of Southern Hemisphere westerly wind intensification from the Pleistocene into the Holocene [*Knudson et al.*,

2011; *Lorrey et al*., 2012], leading to increased terrigenous runoff and sediment yields; however, more work is needed to determine conclusively when and if this acceleration occurred.

Studies of fjords with high accumulation rates near fjord heads have found that these deposits were related to suspended sediment settling from turbid fluvial and glacio-fluvial plumes entering quiescent water off fjord-head deltas [*Bogen*, 1983; *Farrow et al*., 1983]. These deposits would also be expected to decrease in grain diameter away from the fluvial energy source [*Pickrill*, 1993]. Several of the fjord-head (proximal) regions in the fjords sampled in the present study have small river deltas (e.g., Rea and Camelot Rivers in Doubtful Sound and Seaforth River in Dusky Sound), indicative of rapid and localized deposition from fluvial bed load and suspended load. At the distal end of fjords, wave and tidal action may rework material over shallow fjord-mouth sills but gradually decrease in importance landward. This has been observed in Puget Sound [*Geyer and Cannon*, 1982] as well as in Fiordland [*Pickrill*, 1987]. Landslides, common in fjords because of their steep walls, are thought to focus sediment gravitationally into the deep, medial basins of fjords [*Aarseth et al*., 1989; *Bentley and Kahlmeyer*, 2012; *Hjelstuen et al*., 2013]. Other delivery mechanisms identified in fjords to date may produce blanket deposits whose thickness and grain size signature are not dependent on source proximity, such as ice rafting [*Gilbert*, 1983] or autochthonous biological productivity, which is limited by nutrient availability or light [*Schüller and Savage*, 2011]. In the nonglaciated Fiordland areas studied, biological production is the source of the majority of the modern sediment away from fjord heads [*Pickrill*, 1987]. The relatively high LSR we observe in proximal and distal regions suggests that the dominant sediment delivery mechanisms in Fiordland grade between fluvial and tidal inputs at fjord heads and mouths, respectively, with ongoing planktonic biological production throughout the fjord surface waters.

While previous research demonstrates that landslides are an important geomorphic process in southwest New Zealand [*Korup*, 2005], the fact that only 4 of 21 cores show any indications (distorted bedding, uniform excess $^{210}$Pb activity) of landslide-induced stratigraphy within the range of $^{210}$Pb geochronology (100–150 years) suggests that landslides are not a dominant sedimentary depositional process (though they may be important locally) on decadal time scales in these fjord systems. Smaller landslide events from fjord walls may contribute sediment to the fjord basins but cannot be distinguished by $^{210}$Pb and X-radiography from millimeter-scale laminations caused by seasonally variable terrestrial runoff sourcing from the fjord catchment. At longer time scales (e.g., $>$100 years), landslides may provide a mechanism to reconcile the apparent disparity between higher modern rates of sediment accumulation at fjord heads and mouths with the greater thicknesses of sediment accumulation in medial fjord basins. Infrequent, large fjord-wall landslides, when traversing the basin subaqeuously, may remobilize and redistribute sediment from shallower fjord subenvironments, as well as deliver sidewall material into the deepest part of the fjord.

### 4.2. Effects of Fiordland Sediment Delivery Mechanisms on Organic Carbon Burial

If fluvial, tidal, and biological processes are the dominant modern sediment delivery mechanisms in Fiordland, it is important then to consider the fate of OC buried in the fjords by these mechanisms since it differs from modern glaciated fjords and Fiordland earlier in the Holocene. This also provides inferences about how OC burial may evolve globally in fjords with future changes in climate. OC delivered to Fiordland from fluvial sources is terrestrial, with high quantities of woody angiosperm debris and soil OC, shown by biomarker analysis [*Smith et al*., 2010]. In this high OC accumulation setting, there are competing processes for and against the preservation of OC in the sediment. Biological (e.g., bioturbation) and physical (e.g., mass movement) processes which serve to mix or resuspend the sediment encourage the oxidation of OC incorporated in that sediment [*Burell*, 1988; *St-Onge and Hillaire-Marcel*, 2001; *Nuwer and Keil*, 2005]. The delivery mechanism of the OC-bearing sediment is important because it ultimately determines the location and rate of burial, as well as the initial concentration of OC in the sediment, since organic particles are size- and density-sorted during subaqueous transport along with mineral constituents [*Cui et al*., 2016].

Further down-fjord in the medial basins, the OC in Fiordland sediments becomes more marine-derived, as terrigenous sediment inputs are reduced, increasing the relative importance of OC derived from phytoplankton productivity [*Goebel et al*., 2005; *Smith et al*., 2010; *Schüller and Savage*, 2011]. The lower sediment accumulation rates in these areas may not bury OC as quickly, but bio-physical mixing is also reduced in these low-energy, low-oxygen environments [*Schüller et al*., 2015], limiting remineralization. The distal sediments of Fiordland have the highest proportions of marine- and planktonic- derived OC. These sediments may have

preservation potential due to high sediment accumulation rates; however, these areas have high oxidation potential due to wave and tidal mixing with oxygen-rich seawater.

The balance between relative rates of OC burial and decomposition may be illustrated by the differences between Doubtful Sound and Dusky Sound. Doubtful Sound showed an increase in OCAR from proximal site 2201 at the head of the fjord to site 2401 in a medial basin, while Dusky Sound showed a down-fjord decrease from two proximal sites to two distal sites. Doubtful Sound's dendritic catchment planform allows medial basins (like that sampled in core 2401) to be closer to terrestrial sources of high %OC sediment, while Dusky Sound's linear catchment geometry leads to distal and medial sites which are comparatively farther from any fluvial inputs.

### 4.3. Comparison of Fiordland Sediment Delivery and OC Burial With Other Fjords

Some fjords in Chile, Canada, and southern Alaska are in relatively low latitudes, with vegetated catchments, high precipitation rates, and nonglacial fluvial inputs, and may be expected to display similar sediment delivery mechanisms and OC burial to those of Fjordland. Indeed, in Chilean fjords, *Sepúlveda et al*. [2011] found quite similar ranges of OC% (0.5–3.4%), LSR (1.4–7.4 mm/yr), and spatial distribution of terrestrial to marine sources pattern as those in the present study. Similar patterns of LSR and OC burial have also been observed in Québec [*St-Onge and Hillaire-Marcel*, 2001].

Higher-latitude, glaciated fjords in Alaska, Greenland, Scandinavia, Svalbard, and Antarctica lack significant vegetation in their catchments and have highly modulated hydrology (i.e., precipitation is not directly linked to fluvial outflow, due to glacial storage), which results in distinct delivery mechanisms compared with their warmer counterparts. These environments tend to display high mineral sediment accumulation rates at fjord heads (up to 220–365 mm/yr [*Ullrich et al*., 2009; *Walinsky et al*., 2009]) due to turbid glacial rivers and glaciofluvial processes, as well as evidence that ice-rafting and landslide mechanisms can deliver sediment further down-fjord to the deeper basins [*Elverhøi et al*., 1983; *Winkelmann and Knies*, 2005; *Walinsky et al*., 2009; *Bentley and Kahlmeyer*, 2012]. However, higher-latitude fjords tend to have relatively low %OC in sediments, as catchments are not vegetated and OC sources must be autochthonous or marine. Despite the low %OC, OCAR measured in glaciated Alaskan fjords were 1–2 orders of magnitude higher (46–211 mg/cm$^2$/yr [*Walinsky et al*., 2009]) than those measured in Fiordland (1.50–9.23 mg/cm$^2$/yr) due to the rapid mineral sedimentation, presumably coupled with release of lithogenic OC. It might be concluded that with warming climate and disappearance of fjord glaciers, the importance of fjords globally as sites OC burial would decline, with the decreased terrigenous sourcing at higher latitudes outweighing greening effects in the catchment. However, this prediction will likely be complicated by changes in phytoplankton productivity and catchment precipitation change (magnitude and rainfall versus snowfall).

## 5. Conclusions and Implications

In this study, we demonstrate spatial variability in LSR across different depositional regimes within fjords in Fiordland, New Zealand. LSR varies greater than a factor of 10, depending on proximity to sediment sources and sediment-transport energy such as fjord-head streams, fjord-mouth sills, and landslide events. These LSR patterns are spatially distinct from other fjord regions globally and from Fiordland earlier in the Holocene. LSR are highest in the proximal and distal fjord subregions, suggesting that fjord-head streams and marine exchange are the primary controls on LSR in Fiordland, but the importance of other delivery mechanisms, from precipitation-driven "normal" runoff to large landslide failures of steep slopes, cannot be discounted. Modern LSR and OCAR presented in this study are higher than millenial rates previously published for the Fiordland region, which may indicate recent increases in precipitation-induced erosion, transport, and deposition. The variable mineral dilution effect caused by the high spatial variability of LSR is a control on %OC deposited at the fjord substrate. In addition to bottom oxygen availability, mineral LSR is also a control on OCAR, by reducing the time during which OC is exposed to biological decomposition and physical mixing in near-surface sediments.

These relationships may become more complicated in fjord regions worldwide that are subjected to disparate delivery mechanisms (e.g., glaciated fjords where sedimentary material is generated and transported by basal glacial processes, calving of the glacier itself, and sea ice rafting). OCAR measured in this study are similar in magnitude to those measured in nonglaciated fjords in Alaska, Canada, and Chile. Glaciated

fjords appear to have higher potential for long-term OC storage, as the extremely high LSR bury OC where it cannot be decomposed. The results presented here for nonglaciated fjords in New Zealand may become increasingly relevant if future climate warming results in glaciated fjords being transformed into settings similar to lower latitude fjords.

**Acknowledgments**

Thorough descriptions of all field and laboratory method and calculations are given in Supporting Information S1. We thank the University of Otago for a grant awarded to Candida Savage to fund the research cruise and the University of Texas at Austin Jackson School of Geosciences William R. Muehlberger Field Geology Scholarship for international travel funds. Special thanks to Dave Rundgren, Bob Dagg, Bill Dickson, and the crew of the R/V *Polaris II* for field assistance, as well as Dan Duncan and Andrea Hanna at the University of Texas Institute for Geophysics for laboratory assistance.

## References

Aarseth, I., Ø. Lønne, and O. Giskeødegaard (1989), Submarine slides in glaciomarine sediment in some western Norwegian fjords, *Mar. Geol.*, *88*, 1–21.

Allison, M. A., T. S. Bianchi, B. A. McKee, and T. P. Sampere (2007), Carbon burial on river-dominated continental shelves: Impact of historical changes in sediment loading adjacent to the Mississippi River, *Geophys. Res. Lett.*, *34*, L01606, doi:10.1029/2006GL028362.

Bentley, S. J., and E. Kahlmeyer (2012), Patterns and mechanisms of fluvial sediment flux and accumulation in two subarctic fjords: Nachvak and Saglek Fjords, Nunatsiavut, Canada, *Can. J. Earth. Sci.*, *49*, 1200–1215, doi:10.1139/E2012-052.

Berner, R. A. (2003), Overview: The long-term carbon cycle, fossil fuels and atmospheric composition, *Nature*, *426*, 323–326, doi:10.1038/nature02131.

Bianchi, T. S. (2007), *Biogeochemistry of Estuaries*, pp. 103–117, Oxford University Press, Oxford, U. K.

Bogen, J. (1983), Morphology and sedimentology of deltas in fjord and fjord valley lakes, *Sed. Geol.*, *36*, 245–267.

Brewin, P. E., P. K. Probert, and M. F. Barker (2008), Deep-basin macrobenthos of Doubtful Sound, Fiordland, New Zealand, *New Zealand J. Mar. Freshwater Res.*, *42*, 1–21, doi:10.1080/00288330809509932.

Burell, D. C. (1988), Carbon flow in fjords, *Oceanogr. Mar. Biol. Annu. Rev.*, *26*, 143–226.

Cui, X., T. S. Bianchi, J. A. Hutchings, C. Savage, and J. H. Curtis (2016), Partitioning of organic carbon in surface sediments of Fiordland, New Zealand, *J. Geophys. Res.: Biogeosciences*, *121*, 1016–1031.

Elverhøi, A., Ø. Lonne, and R. Seland (1983), Glaciomarine sedimentation in a modern fjord environment, Spitsbergen, *Polar Res.*, *1*, 127–149.

Farrow, G. E., J. P. M. Syvitski, and V. Tunnicliffe (1983), Suspended particulate loading on the Macrobenthos in a highly turbid fjord: Knight Inlet, British Columbia, *Can. J. Fish. Aquat. Sci.*, *40*, 273–288.

Geyer, W. R., and G. A. Cannon (1982), Sill processes related to deep water renewal in a fjord, *J. Geophys. Res.*, *87*, 7985–7996, doi:10.1029/JC087iC10p07985.

Gilbert, R. (1983), Sedimentary processes of Canadian Arctic fjords, *Sed. Geol.*, *36*, 147–175.

Goebel, N. L., S. R. Wing, and P. W. Boyd (2005), A mechanism for onset of diatom blooms in a fjord with persistent salinity stratification, *Estuarine Coastal Shelf Sci.*, *64*, 546–560.

Hancox, G. T., and N. D. Perrin (2009), Green Lake Landslide and other giant and very large postglacial landslides in Fiordland, New Zealand, *Quat. Sci. Rev.*, *28*, 1020–1036, doi:10.1016/j.quascirev.2008.08.017.

Hein, F. J., and F. P. M. Syvitski (1992), Sedimentary environments and facies in an arctic basin, Itirbilung Fiord, Baffin Island, Canada, *Sed. Geol.*, *81*, 17–45.

Hinojosa, J. L., C. M. Mow, C. H. Stirling, G. S. Wilson, and T. I. Eglinton (2014), Carbon cycling and burial in New Zealand's fjords, *Geochem. Geophys. Geosyst*, *15*, 4047–4063, doi:10.1002/2014GC005433.

Hjelstuen, B. O., H. Kjennbakken, V. Bleikli, R. A. Ersland, S. Kvilhaug, C. Euler, and S. Alvheim (2013), Fjord stratigraphy, and processes—Evidence from the NE Atlantic Fensfjorden system, *J. Quat. Sci.*, *28*, 421–432, doi:10.1002/jqs.2636.

Inall, M. E., and P. A. Gillibrand (2010), The physics of mid-latitude fjords: A review, in *Fjord Systems and Archives*, *Geological Society of London Special Publications*, vol. 344, edited by J. A. Howe et al., pp. 17–33, doi: 10.1144/SP344.3.

Knudson, K. P., I. L. Hendy, and H. L. Neil (2011), Re-examining Southern Hemisphere westerly wind behavior: Insights from a late Holocene precipitation reconstruction using New Zealand fjord sediments, *Quat. Sci. Rev.*, *30*, 3124–3138, doi:10.1016/j.quascirev.2011.07.017.

Korup, O. (2005), Distribution of landslides in southwest New Zealand, *Landslides*, *2*, 43–51, doi:10.1007/s10346-004-0042-0.

Land Information New Zealand (2001), Western approaches to Foveaux Strait, Chart NZ 76. [Available at https://data.linz.govt.nz/layer/1263-chart-nz-76-western-approaches-to-foveaux-strait/.]

Lorrey, A. M., et al. (2012), Palaeocirculation across New Zealand during the last glacial maximum at ~21 ka, *Quat. Sci. Rev.*, *36*, 189–213, doi:10.1016/j.quascirev.2011.09.025.

Mackenzie, F. T., and A. Lerman (2010), *Carbon in the Geobiosphere—Earth's Outer Shell*, pp. 402, Springer, Dordrecht, Netherlands.

Nittrouer, C. A., R. W. Sternberg, R. Carpenter, and J. T. Bennett (1979), The use of Pb-210 geochronology as a sedimentological tool: Application to the Washington continental shelf, *Mar. Geol.*, *31*, 297–316.

Noller, J. S. (2000), Lead-210 geochronology, in *Quaternary Geochronology: Methods and Applications*, edited by J. S. Noller, J. M. Sowers, and W. R. Letts, pp. 115–120, AGU Reference Shelf 4, Washington, D. C.

Nuwer, J. M., and R. G. Keil (2005), Sedimentary organic matter geochemisty of Clayoquot Sound, Vancouver Island, British Columbia, *Limnol. Oceanogr.*, *50*, 1119–1128.

Pickard, G. L., and B. R. Stanton (1980), Pacific fjords—A review of their water characteristics, in *Fjord Oceanography*, edited by H. J. Freeland, D. M. Farmer, and C. D. Levings, pp. 1–50, Lenum Press, New York.

Pickrill, R. A. (1987), Circulation and sedimentation of suspended particulate matter in New Zealand fjords, *Mar. Geol.*, *74*, 21–39.

Pickrill, R. A. (1993), Sediment yields in Fiordland, *J. Hydrol. (N.Z.)*, *31*, 39–55.

Pickrill, R. A., J. M. Fenner, and M. S. McGlone (1992), Late Quaternary evolution of a fjord environment in Preservation Inlet, New Zealand, *Quat. Res.*, *38*, 331–346.

Powell, R. D., and B. F. Molnia (1989), Glacimarine sedimentary processes, facies and morphology of the south-southeast Alaska shelf and fjords, *Mar. Geol.*, *85*, 359–390.

Sansom, J. (1984), *The Climate and Weather of Southland*, *New Zealand Meteorological Service Miscellaneous Publication 115(15)*, pp. 14, Wellington, New Zealand.

Schüller, S. E., M. A. Allison, T. S. Bianchi, F. Tian, and C. Savage (2013), Historical variability in past phytoplankton abundance and composition in Doubtful Sound, New Zealand, *Cont. Shelf Res.*, *69*, 110–122, doi:10.1016/j.csr.2013.09.021.

Schüller, S. E., T. S. Bianchi, X. Li, M. A. Allison, and C. Savage (2015), Historical reconstruction of phytoplankton composition in estuaries of Fiordland, New Zealand: The application of plant pigment biomarkers, *Estuar Coasts*, *38*, 56–71, doi:10.1007/s12237-014-9771-z.

Schüller, S. E., and C. Savage (2011), Spatial distribution of diatom and pigment sedimentary records in surface sediments in Doubtful Sound, Fiordland, New Zealand, *NZ J. Mar. Freshw. Res.*, *45*, 591–608, doi:10.1080/00288330.2011.561865.

Sepúlveda, J., S. Pantoja, and K. A. Hughen (2011), Sources and distribution of organic matter in northern Patagonia fjords, Chile (~44-47°S): A multi-tracer approach for carbon cycling assessment, *Cont. Shelf Res.*, *31*, 315–329, doi:10.1016/j.csr.2010.05.013.

Smith, R. W., T. S. Bianchi, M. A. Allison, C. Savage, and V. Galy (2015), High rates of organic carbon burial in fjord sediments globally, *Nat. Geosci.*, *8*, 450–453, doi:10.1038/ngeo2421.

Smith, R. W., T. S. Bianchi, and C. Savage (2010), Comparison of lignin phenols and branched/isoprenoid tetraethers (BIT index) as indices of terrestrial organic matter in Doubtful Sound, Fiordland, New Zealand, *Org. Geochem.*, *41*, 281–290, doi:10.1016/j.orggeochem.2009.10.009.

St-Onge, G., and C. Hillaire-Marcel (2001), Isotopic constraints of sedimentary inputs and organic carbon burial rates in the Saguenay Fjord, Quebec, *Mar. Geol.*, *176*, 1–22, doi:10.1016/S0025-3227(01)00150-5.

Syvitski, J. P. M., and J. W. Murray (1981), Particle interaction in fjord suspended sediment, *Mar. Geol.*, *39*, 215–242.

Syvitski, J. P. M., K. W. Asprey, D. A. Clattenburg, and G. D. Hodge (1985), The prodelta environment of a fjord: Suspended particle dynamics, *Sedimentology*, *32*, 83–107, doi:10.1111/j.1365-3091.1985.tb00494.x.

Syvitski, J. P. M., K. W. G. LeBlanc, and R. E. Cranston (1990), The flux and preservation of organic carbon in Baffin Island fjords, in *Glacimarine Environments*: *Processes and Sediments*, edited by J. A. Dowdeswell and J. D. Scourse, *Geol. Soc. Spec. Pub. 53*, 177–199.

Ullrich, A. D., E. A. Cowan, S. D. Zellers, J. M. Jaeger, and R. D. Powell (2009), Intra-annual variability in benthic foraminiferal abundance in sediments of Disenchantment Bay, an Alaskan glacial fjord, *Arct. Antarct. Alp. Res.*, *41*, 257–271, doi:10.1657/1938-4246-41.2.257.

Walinsky, S. E., F. G. Prahl, A. C. Mix, B. P. Finney, J. M. Jaeher, and G. P. Rosen (2009), Distribution and composition of organic matter in surface sediments of coastal Southeast Alaska, *Cont. Shelf Res.*, *29*, 1565–1579, doi:10.1016/j.csr.2009.04.006.

Winkelmann, D., and J. Knies (2005), Recent distribution and accumulation of organic carbon on the continental margin west off Spitsbergen, *Geochem. Geophys. Geosyst.*, *6*, Q09012, doi:10.1029/2005GC000916.